



Published in final edited form as:

Circulation. 2009 January 20; 119(2): 269–280. doi:10.1161/CIRCULATIONAHA.108.773424.

Pressure-Overload Induced Alterations in Fibrillar Collagen Content and Myocardial Diastolic Function: Role of SPARC in Post-Synthetic Procollagen Processing

Amy D. Bradshaw, Ph.D., Catalin F. Baicu, Ph.D., Tyler J. Rentz, BS, An O. Van Laer, MS, Janet Boggs, BS, John M. Lacy, BS, and Michael R. Zile, M.D.

Gazes Cardiac Research Institute, Division of Cardiology, Department of Medicine, RHJ Department of Veterans Affairs Medical Center, Medical University of South Carolina, Charleston, SC

Abstract

Background—Chronic pressure-overload (PO) causes myocardial hypertrophy, increased fibrillar collagen content, and abnormal diastolic function. We hypothesized that one determinant of these PO-induced changes is the extracellular processing of newly synthesized procollagen into mature collagen fibrils. We further hypothesized that SPARC (Secreted Protein Acidic and Rich in Cysteine) plays a key role in post-synthetic procollagen processing in normal and PO myocardium.

Methods & Results—To determine whether PO-induced changes in collagen content and diastolic function are affected by the absence of SPARC, age-matched wild-type (WT) and SPARC null mice underwent either transverse aortic constriction (TAC) for 4 weeks or served as non-operated controls (Control). Left ventricular (LV) collagen content was measured histologically by collagen volume fraction (CVF), collagen composition was measured by hydroxyproline assay as soluble collagen (1M NaCl extractable) vs. insoluble collagen (mature cross-linked), and collagen morphologic structure was examined by scanning electron microscopy. SPARC expression was measured by immunoblot. LV, myocardial, and cardiomyocyte structure and function were assessed using echocardiographic, papillary muscle and isolated cardiomyocyte studies. In WT mice, TAC increased LV mass, SPARC expression, myocardial diastolic stiffness, fibrillar collagen content, soluble, and insoluble collagen. In SPARC null mice, TAC increased LV mass to an extent similar to WT mice. In addition, in SPARC Null mice TAC increased fibrillar collagen content but significantly less than that seen in WT TAC mice. Furthermore, the proportion of LV collagen which was insoluble was less in the SPARC Null TAC mice (86±2%) compared with the WT TAC mice (99±2%, $p < 0.05$) and the proportion of collagen which was soluble was greater in the SPARC Null TAC mice (14±2%) compared with the WT TAC mice (1±2%, $p < 0.05$). As a result, myocardial diastolic stiffness was lower in the SPARC Null TAC mice (0.075±0.005) than in WT TAC mice (0.045±0.005, $p < 0.05$).

Conclusions—The absence of SPARC reduced PO-induced alterations in ECM fibrillar collagen and diastolic function. These data support the hypothesis that SPARC plays a key role in post-synthetic procollagen processing and the development of mature cross-linked collagen fibrils in normal and pressure-overloaded myocardium.

Address for Correspondence and Reprint Requests: Amy D. Bradshaw, Ph.D. Medical University of South Carolina Department: Medicine Division: Cardiology 114 Doughty Street, Room 223 Gazes / Strom Thurmond Research Building Charleston, South Carolina, 29425 Phone: 843-792-4959, Fax: 843-876-5068 bradshad@musc.edu.

Disclosures: None

Keywords

Collagen; SPARC; Hypertrophy; Pressure-overload; Diastolic function

Chronic pressure overload, such as occurs with arterial hypertension, is a common cause of left ventricular (LV) remodeling and frequently leads to the development of chronic heart failure (CHF) (1–3). Pressure-overload induced remodeling is characterized by the development of cardiomyocyte hypertrophy, an increase in extracellular matrix (ECM) fibrillar collagen content and the development of abnormal diastolic function (3–6). However, the mechanisms by which pressure-overload leads to cardiac remodeling, particularly a net increase in myocardial collagen content and the development of diastolic dysfunction, have not been completely defined.

Fibrillar collagen biosynthesis begins within a fibroblast with the synthesis of procollagen α chain monomeric proteins which then form the triple helical structure of a procollagen molecule (7) (Figure 1). After synthesis, a procollagen molecule is secreted into the extracellular space where it must undergo a series of ordered, time sensitive, and location sensitive processing steps to become a mature cross-linked insoluble structural collagen fibril. We hypothesized that one fundamental mechanism by which chronic pressure-overload increases myocardial fibrillar collagen content and causes the development of abnormal diastolic function is an alteration in post-synthetic procollagen processing. We further hypothesized that one determinant of post-synthetic procollagen processing is the extracellular protein, SPARC (Secreted Protein Acidic and Rich in Cysteine).

Previous studies in non-cardiovascular tissues have shown that SPARC is a procollagen-binding protein with counter-adhesive activity, participates in the coordination of procollagen processing and facilitates the formation and assembly of mature cross-linked insoluble structural collagen fibrils (8,9). Studies in dermal tissue and dermal fibroblasts support the hypothesis that when SPARC binds to newly secreted procollagen, it chaperones the procollagen molecule through processing steps within the extracellular space (Figure 1), and limits binding of procollagen to cell surface receptors (10–13). By diminishing procollagen engagement of cell surface receptors, SPARC facilitates the optimal sequence and timing of the processing steps and prevents procollagen from being prematurely degraded or improperly processed (10). SPARC is not absolutely required to process procollagen but SPARC enhances and facilitates procollagen processing. In transgenic mice that do not express SPARC (SPARC Null), there was a substantial decrease in dermal collagen concentration, collagen fibrils were significantly smaller, and the dermis had a significantly decreased tensile strength (and decreased stiffness) compared with dermis from wild-type (WT) mice (11).

However, post-synthetic procollagen processing has not been extensively studied in myocardial tissue. It is not known whether SPARC is an important determinant of post-synthetic procollagen processing in the myocardium or whether procollagen processing is altered in the myocardium of the pressure-overloaded left ventricle. It is also not known whether a change in SPARC expression is a fundamental mechanism by which pressure-overload increases myocardial fibrillar collagen content and causes diastolic dysfunction. Accordingly, the purpose of this study was to test the hypothesis that: 1) SPARC is an important determinant of myocardial fibrillar collagen content in normal myocardium, 2) SPARC is significantly increased in pressure-overload myocardium, and 3) the absence of SPARC significantly alters the effects of pressure-overload on myocardial fibrillar collagen content and diastolic function.

Methods

Protocol

Four groups of mice were studied (WT control, WT transverse aortic constriction [TAC], SPARC-Null control, SPARC Null TAC) using four protocols (A–D) (Figure 2). Transgenic mice that do not express SPARC (SPARC Null, produced by targeted gene deletion) were made on a C57Bl6/SV129 background. SPARC Null mice were compared to their wild-type littermate mice (C57Bl6/SV129) both in the control state and after TAC. To determine whether the absence of SPARC resulted in a change in cardiac phenotype, non-operated WT and SPARC Null control mice underwent echocardiography and then were randomly assigned to 1 of 4 experimental protocols: A–D. To determine whether the absence of SPARC altered the phenotypic response to TAC-induced PO, WT mice and compared to SPARC Null mice underwent TAC four weeks followed by echocardiography and random assignment to 1 of 3 experimental protocols: A–C. The methods used to perform echocardiography (14) and TAC have been previously described and are presented in detail in our electronic supplement.

Twenty-nine non-operated Control SPARC-null mice (16 males, 13 females) and 29 WT (15 males, 14 female) mice were studied at 12 weeks of age and were entered into protocols A (n=10 SPARC Null, 10 WT), B (n=7 SPARC Null, 7 WT), C (n=6 SPARC Null, 6 WT), and D (n=6 SPARC Null, 6 WT).

Forty-three SPARC-null (22 male, 21 female) and 42 WT (22 male, 20 female) mice were subjected to TAC surgery at 12 weeks of age. Twenty six SPARC-null (14 male, 12 female) and 18 WT (10 male, 8 female) mice survived 4 weeks of TAC and were entered into protocols A (n=14 SPARC null, 8 WT), B (n=6 SPARC null, 5 WT) and C (n=6 SPARC null, 6 WT).

All procedures performed were approved by the MUSC IACUC committee in accordance with NIH guidelines.

Protocol A—Mice were anesthetized using inhalation isoflurane, given 200 units of heparin IP, the LV was isolated, weighed, divided into 2 pieces and frozen in liquid nitrogen. Two sets of analyses were performed: 1- Collagen composition was determined by biochemistry; 2- SPARC abundance was determined by immunoblot.

Extraction and Biochemical quantification of Collagen: Frozen LV tissue was lyophilized, weighed (dry weight), pulverized, resuspended in 1M NaCl with protease inhibitors, tumbled overnight at 4° C and centrifuged. The supernatant then contained the “NaCl soluble” collagen (i.e., largely non-cross-linked collagen); the pellet contained the “NaCl insoluble” collagen (fully mature cross-linked fibrillar collagen). Each collagen fraction was processed separately. Collagen fractions underwent complete acid hydrolysis with 6 N HCl for 18 hours at 120°C, and then each was neutralized to pH7 with 4N NaOH. One ml of Chloramine T was added to 2 ml volumes of collagen sample, and incubated at room temperature for 20 minutes. One ml of Ehrlich's Reagent (60% perchloric acid, 15 ml 1-propanol, 3.75 g p-dimethyl-amino-benzaldehyde in 25 ml) was added and samples were incubated at 60°C for 20 minutes. Absorbance at 558 λ was read on a spectrophotometer. Collagen was quantified as μg hydroxyproline per mg dry weight LV myocardium. Total collagen was calculated as the sum total of the NaCl soluble and insoluble fractions. Thus, three collagen measurements were made by this hydroxyproline quantification of differentially isolated collagen fractions: NaCl insoluble collagen (mature, fully processed, cross-linked collagen) and NaCl soluble collagen (not processed or incompletely processed but non cross-linked collagen) and total collagen (the sum of soluble plus insoluble collagen).

Western Blot Analysis: Immunoblots were performed on LV tissue samples extracted with 1M NaCl to obtain the salt soluble fraction or LV tissue samples treated with triton extraction buffer. SDS-PAGE gels were probed with murine anti-SPARC polyclonal antibodies (1:20,000 dilution, R&D Systems, Minneapolis, MN).

Protocol B—Mice were anesthetized, given 200 units of heparin IP, the LV isolated, the aorta cannulated, the LV perfused with BDM, and the papillary muscle was isolated to determine *in vitro* myocardial systolic and diastolic function.

Papillary Muscle Preparation and Myocardial Function Measurements: Previously, our laboratory performed isolated papillary muscle studies in normal and pressure-overload cats and rats (15–17). The methods used in these studies were modified in order to study murine papillary muscles (please electronic supplement). Passive diastolic stiffness was examined two ways: 1) define rest stress at L_{max} and 2) perform a muscle stretch at a very slow stretch rate (1 mm/min) beginning from near slack length (very lightly preloaded muscle at 0.1 g) to a muscle length of 15% greater than that at slack length (equivalent to L_{max} preload). The myocardial stress vs. strain relationship during this muscle stretch were used to calculate the passive stiffness constant, β , as $Stress = Ae^{(\beta Strain)} + C$. Myocardial stress was calculated from muscle force divided by muscle cross-sectional area and strain was calculated as $(L - L_0) / L_0$ where L = muscle length during stretch and L_0 = muscle length at 0.1 g preload.

Protocol C—Mice were anesthetized, given 200 units of heparin IP, the LV isolated, the aorta cannulated, the LV was divided in half. One half of the left ventricle was fixed in 4% paraformaldehyde and stored in 4% paraformaldehyde at 4 °C to undergo quantitative collagen content analysis using light microscopy studies. The other half of the left ventricle was fixed in 2% glutaraldehyde to undergo morphometric analysis of fibrillar collagen using scanning electron microscopy studies

Collagen Content by Light Microscopy: LV sections were stained with picrosirius red (PSR) to detect collagen fibers and viewed with polarized light under dark field optics to detect birefringence of collagen fibers. Quantitative analysis of PSR stained images captured with polarized light were performed. Five fields chosen at random from each mouse were scanned using Sigma Scan software. Fields with large blood vessels were excluded from the analysis. Areas examined were distributed throughout the myocardium from subendocardial to subepicardial and excluded the epicardial surface. Collagen volume fraction (CVF) was calculated as the area stained by PSR divided by the total area of interest using previously published techniques (18) PSR birefringent staining was used to identify and quantify mature fully processed cross-linked insoluble fibrillar collagen within the myocardium (19,20). Additional studies confirmed that PSR birefringent staining does not detect procollagen and is specific for mature collagen fibrils are presented in the electronic supplement.

Collagen Morphologic Structure by Scanning Electron Microscopy: LV samples were processed using previously published techniques which included immersion fixation in 2% Cacodylate Glutaraldehyde, post fixation in 2% Osmium Tetroxide, dehydration with 100% alcohol, drying with Hexamethyldisilazine using a Critical Point Dryer (21). Samples were mounted on scanning electron microscopy (SEM) stubs, sputter coated with gold palladium and imaged using a JEOL JSM-5410 scanning microscope at 15 KV, with Lens Current at 46 and the working distance at 14.

Protocol D—Tail cuff arterial blood pressure was measured, then LV cardiomyocytes were isolated using collagenase techniques and cardiomyocyte systolic and diastolic function were assessed. Mice Blood pressure (BP) was obtained using a noninvasive tail cuff (BP2000

system, VisiTech) (22). BP measurements were used together with echocardiographically determined LV stroke volume to calculate effective arterial elastance (E_a) (23) Briefly, $E_a = \text{systolic pressure} / \text{Stroke Volume (SV)}$, where $SV = \text{end diastolic volume} - \text{end systolic volume}$. After the blood pressure and echocardiographic studies, the mice underwent cardiomyocytes isolation.

Cardiomyocyte Isolation and Function Measurements: Cardiomyocyte isolation was performed using collagenase digestion methods (24, please see electronic supplement). Using methods described below, 20 cardiomyocytes from each mouse underwent study to examine cardiomyocytes systolic and diastolic properties using the IonOptix system and 10 cardiomyocytes from each mouse underwent study to examine cardiomyocytes passive stiffness using our custom stretch system.

Cardiomyocyte systolic and diastolic relaxation properties were measured in isolated cardiomyocytes using the IonOptix system (IonOptix, Milton, MA) (25, please see electronic supplement).

Cardiomyocyte passive stiffness properties of isolated cardiomyocytes were determined using a passive stretch method (26, please see electronic supplement).

Statistical Analysis

Data are presented as mean \pm SEM. Differences in continuous variables between the WT control, WT TAC, SPARC null control and SPARC null TAC groups were determined using one way analysis of variance (ANOVA) followed by Tukey testing of pair-wise analysis. While data comparing WT control vs. SPARC Null control are presented in the results section separately from data comparing WT TAC vs. SPARC Null TAC, all comparisons were done in the context of a four group comparison (WT control, WT TAC, SPARC Null control, SPARC Null TAC) using the statistical methods stated above. Differences in dichotomous variables were determined using X^2 test, adjustment for multiple comparisons was made using Bonferonni methods for testing of pair wise differences which has a similar relative conservative approach to that used with the continuous variables. The survival data presented in Figure 3 utilized a standard Kaplan-Meier analysis. A p value of <0.05 was considered significant. The primary outcome variable for this study was the concentration of insoluble collagen measured by biochemically determined hydroxyproline levels. The other measurements presented are secondary endpoints that are included as an exploratory analysis to examine pathophysiological mechanisms. The authors had full access to and take full responsibility for the integrity of the data. All authors have read and agree to the manuscript as written.

Results

SPARC Null Mouse Cardiac Phenotype

Fibrillar Collagen content by light microscopy—There was a significant decrease in PSR staining in SPARC Null LV myocardium compared with that seen in the WT control LV myocardium (Figure 4). CVF (Figure 4) was decreased in the SPARC Null control (0.46 ± 0.04 %) compared to the WT control (0.92 ± 0.10 %, $p < 0.05$).

Collagen composition by biochemistry—In SPARC Null control mice, there was a decrease in total collagen and a decrease in the relative proportion of collagen that was insoluble compared with WT control mice (Figure 4). The relative proportion of insoluble collagen fell from $91 \pm 1\%$ in WT to $87 \pm 1\%$ in SPARC Null ($p < 0.05$), Table 2. By contrast, the relative

proportion of collagen that was soluble increased from $9 \pm 1\%$ in WT to $13 \pm 1\%$ in SPARC Null ($p < 0.05$).

Collagen morphology by scanning EM—Morphologic structure and distribution of fibrillar collagen was qualitatively examined in LV samples from WT and SPARC-Null control mice (Figure 4). Fibrillar collagen struts and weave were reduced in the SPARC-Null mice.

LV Structure and Function—There were no significant differences in LV volume, mass, mass/body weight ratio, volume/mass ratio, or ejection fraction in SPARC Null mice compared to WT mice (Table 1). Thus, the absence of SPARC did not alter LV volume, geometry, mass or systolic function.

Vascular Function—The absence of SPARC did not significantly affect blood pressure or effective arterial elastance. Systolic blood pressure was 102 ± 7 in WT vs. 104 ± 6 mmHg in SPARC Null and effective arterial elastance was 2.3 ± 0.3 in WT vs. 2.4 ± 0.2 mmHg / μL in SPARC Null. There were no significant differences in any of these measurements between WT and SPARC Null control mice.

Myocardial function—The effects of the absence of SPARC on myocardial systolic properties, diastolic relaxation and passive stiffness were assessed using isolated papillary muscle studies. As shown in Table 3, myocardial systolic properties were not significantly different in SPARC Null control mice compared with WT control mice. Similarly, there were no significant differences in myocardial relaxation rates. By contrast, myocardial passive stiffness was decreased in the SPARC Null control mice compared to the WT control mice (Figure 5). The myocardial stiffness constant (β) was significantly decreased in papillary muscles isolated from the SPARC Null mice compared with WT mice (Figure 5).

Cardiomyocyte function—Cardiomyocyte systolic properties as measured by the percent and rate of shortening were not significantly different in SPARC Null vs. WT control cardiomyocytes (Table 3). In addition, cardiomyocyte diastolic properties as measured by the rate of lengthening and cardiomyocytes stiffness were not significantly different in SPARC Null vs. WT control cardiomyocytes.

Effects of TAC

The 28 day survival rates using Kaplan Myer survival curves for the 4 groups of mice studied: WT control, WT TAC, SPARC Null control and SPARC Null TAC are presented in Figure 3. This analysis showed that the procedural and peri-procedural death rate after TAC was similar in the WT and SPARC Null mice; the late survival after TAC was also similar in the WT and SPARC Null mice. There were no deaths in the control groups over 28 days.

SPARC Immunoblot—There was a significant increase in SPARC expression in WT mice 4 weeks after TAC measured in both salt-soluble and detergent-soluble LV myocardial tissue samples (Figure 6). As expected, there was no SPARC expression in SPARC Null mice.

Fibrillar Collagen content by light microscopy—There was a significant increase in PSR staining in WT mice after TAC (Figure 4 C, D). There was also an increase in PSR staining in SPARC Null mice after TAC. However, the increase in PSR staining in SPARC Null TAC mice was less than that which occurred after TAC in WT mice. CVF was increased in the WT TAC ($4.8 \pm 0.8\%$, $p < 0.05$ vs. WT control); CVF was increased in the SPARC Null TAC ($1.49 \pm 0.13\%$, $p < 0.05$ vs. SPARC Null control) however, this TAC induced increase in CVF was less in the SPARC Null TAC than in the WT TAC ($p < 0.05$). The co-efficient of variability between LV regions in the 2 groups of mice was low.

Collagen Composition by biochemistry—*In WT mice*, TAC increased total collagen and increased the relative proportion of collagen that was insoluble (Figure 4). Relative insoluble collagen increased to $99 \pm 2\%$ in WT TAC mice ($p < 0.05$ vs. Control WT mice), Table 2. However, in WT mice, TAC decreased the relative proportion of collagen that was soluble. Relative soluble collagen decreased to $1 \pm 2\%$ in WT TAC mice ($p < 0.05$ vs. WT control mice). *In SPARC Null mice*, TAC resulted in an increase in total collagen compared to SPARC Null control mice, and this increase was similar in extent to the increase in total collagen that occurred in WT mice after TAC (Figure 4). In SPARC Null mice, TAC increased both insoluble and soluble collagen concentrations compared to SPARC Null Control mice. In addition, the relative proportion of collagen that was insoluble ($86 \pm 2\%$) and the relative proportion of collagen that was soluble ($14 \pm 2\%$) were not changed after TAC in the SPARC-Null mice compared to the SPARC Null Control mice (Table 2). However, after TAC, the relative proportion of collagen that was insoluble was smaller and the relative proportion of collagen that was soluble was larger in the SPARC-Null mice compared with the WT control mice (both $p < 0.05$ SPARC-Null TAC vs. WT TAC mice).

Collagen morphology by scanning EM—Morphologic structure and distribution of fibrillar collagen was qualitatively examined in LV samples from WT and SPARC-Null TAC mice (figure 4). In both WT and SPARC Null TAC mice the fibrillar collagen struts and weave were increased compared to control mice; however, these changes were less pronounced in the SPARC-Null mice compared to the WT mice.

LV Structure and Function—TAC-induced PO resulted in an equivalent increase in the LV mass in WT and SPARC Null mice (Table 1). LV mass, wall thickness and relative wall thickness increased in both WT and SPARC Null mice as a result of TAC for 4 weeks. The aortic pressure gradient created by the TAC was increased to an equivalent degree in both the WT and SPARC Null mice after TAC. The aortic gradient reflects the pressure overload “stimulus” created by TAC. This stimulus was similar in both WT and SPARC Null mice that underwent TAC.

Myocardial function—Papillary muscle cross sectional area (CSA) was not affected by the absence of SPARC in the control mice (CSA = 0.41 ± 0.07 mm² in WT vs. 0.43 ± 0.04 in SPARC Null) or the TAC mice (CSA = 0.53 ± 0.04 in WT vs. 0.58 ± 0.04 SPARC Null); however, the CSA was larger in the TAC vs. control mice ($p < 0.05$). Minimum myocardial papillary muscle stress at L_{max} was lower in the SPARC Null mice compared to the WT both in control (4.88 ± 0.2 WT control vs. 3.05 ± 0.35 mN/mm² in SPARC Null control, $p < 0.05$) and after TAC (7.06 ± 0.44 in WT TAC vs. 5.26 ± 0.81 mN/mm² in SPARC Null TAC, $p < 0.05$) however, the minimum myocardial papillary muscle stress at L_{max} was higher in the TAC vs. control mice ($p < 0.05$). Myocardial diastolic stiffness (β) was increased in WT TAC mice compared to Control WT mice. Myocardial diastolic stiffness also increased in TAC SPARC Null mice compared to Control SPARC Null mice; however, this increase was significantly less than that which occurred in WT mice after TAC (Figure 5).

Discussion

The current studies demonstrated that: 1) SPARC Null mice have a significant change in cardiac phenotype compared with WT mice which was characterized by a decrease in mature cross-linked insoluble collagen fibrils and a decrease in myocardial diastolic stiffness, 2) TAC-induced PO in WT mice increased SPARC expression, increased insoluble collagen and increased myocardial stiffness, and 3) TAC-induced PO in SPARC null mice resulted in a significantly smaller increase in insoluble collagen and myocardial stiffness compared to TAC-induced PO in WT mice. These data support the hypothesis that SPARC is an important determinant of post-synthetic procollagen processing and the development of mature cross-

linked collagen fibrils in the normal myocardium and that SPARC is one fundamental determinant by which chronic pressure-overload increases myocardial fibrillar collagen content and contributes to the development of diastolic dysfunction.

Procollagen Processing in Non-Cardiovascular Tissues

After synthesis, procollagen molecules are secreted into the extracellular space where they must undergo a series of ordered, time sensitive, and location sensitive processing steps to become a mature cross-linked insoluble structural collagen fibril (27) (Figure 1). These procollagen processing steps appear to be most efficient and effective in leading to formation of or incorporation into a mature cross-linked insoluble structural collagen fibril when they occur in the presence of “matricellular” proteins such as SPARC (8,9,27). The hypothesis that SPARC coordinates procollagen processing and facilitates collagen fibril assembly and formation (9) is based largely on studies performed in the dermis from normal wild-type and SPARC Null mice. These experiments demonstrated that SPARC-null mice had substantial decreases in dermal collagen concentrations (half that of WT dermis). Collagen fibrils from the dermis of SPARC Null mice were significantly smaller and had a decreased range of fibril diameters compared with the dermis from WT mice (11). In addition, these structural changes in collagen fibrils were associated with changes in the mechanical and functional properties of the dermis including decreased tensile strength (and decreased stiffness) (11).

In experimental models of dermal injury and fibrosis, SPARC Null mice had a significantly blunted response to the fibrotic stimulus with significantly less fibrillar collagen deposition than WT mice (12,13). For example, when foreign material is implanted in the skin, a fibrous capsule is synthesized around the foreign material. In SPARC Null mice, the fibrillar collagen surrounding the foreign material exhibited fewer and smaller diameter fibrils compared to WT mice (13).

Therefore, there is convincing evidence that SPARC is an important determinant of post-synthetic procollagen processing and the development of mature cross-linked collagen fibrils in the ECM of dermal, pulmonary, skeletal, and renal tissues particularly in response to injury. Based on these studies in non-cardiovascular tissues, we hypothesized that procollagen processing and the development of mature cross-linked collagen fibrils would be altered in myocardial tissues of SPARC Null mice and that the response to a stimulus which increases myocardial fibrillar collagen content would be altered in SPARC Null mice.

Proposed Mechanisms by which SPARC Affects Procollagen Processing

The mechanism by which SPARC influences procollagen processing has been studied *in vitro* using primary dermal fibroblast cultures from WT and SPARC Null mice (10). Procollagen, collagen intermediates and soluble and insoluble collagen were measured in the conditioned media and in the “cell associated layer”. In the absence of SPARC, procollagen secreted from fibroblasts had a greater tendency to associate with and bind to the fibroblast cell surface, to undergo either degradation or premature, disordered processing and did not efficiently or effectively develop into mature cross-linked collagen fibrils. If recombinant SPARC (rSPARC) was added to SPARC-null primary fibroblasts cultures, procollagen processing was restored toward normal. When rSPARC was added to SPARC-null fibroblasts, procollagen binding to or association with the fibroblast cell surface was decreased and effective procollagen processing into mature collagen fibrils was returned to levels comparable to the WT fibroblasts (10).

Therefore, these *in vitro* results suggest that SPARC limits procollagen binding to cell surface receptors and promotes processing of procollagen to mature collagen fibrils. In the absence of SPARC, the regulation of procollagen processing is disrupted, collagen interaction with

receptors is enhanced leading to increased degradation of procollagen at the expense of incorporation of processed collagen into insoluble collagen fibrils.

Myocardial Collagen: Effects of the absence of SPARC

LV myocardial collagen was examined in the current study using three independent methods: 1) collagen content was examined using light microscopy PSR birefringent staining and quantified by measuring CVF, 2) collagen composition was examined using biochemically determined hydroxyproline assay to quantify insoluble vs. soluble collagen, and 3) collagen morphology was examined by scanning electron microscopy. These data showed that the absence of SPARC reduced the pressure-overload induced increase in myocardial collagen content, changed the composition of myocardial collagen in favor of more soluble and less insoluble collagen, and altered the collagen morphology. Although the differences in collagen volume fraction were directionally similar to the hydroxyproline analysis, the magnitude of the change in fibrillar collagen as measured by CVF differed somewhat from the biochemically derived collagen measurements made by hydroxyproline analysis. When collagen content was assessed by CVF there was a more robust response to TAC induced POH in mice than was measured by the hydroxyproline analysis. We attribute this difference in collagen measurement to at least three factors. First, the hydroxyproline analysis included measurement of all of the collagen in the left ventricle including that found in association with large blood vessels and the epicardial surface. We do not believe that the absence of SPARC changes collagen associated with large blood vessels and the epicardial surface, therefore the affects of the absence of SPARC on myocardial fibrillar collagen would be somewhat minimized (or perhaps underestimated) by the hydroxyproline analysis. By contrast, CVF measurements were restricted to changes in interstitial collagen and excluded large blood vessels and the epicardial surface. Second, the hydroxyproline assay measured all collagen types not just those which contribute to interstitial fibrillar collagen. By contrast, CVF primarily quantified collagen types I and III that constitute interstitial fibrillar collagen. Third, CVF measurements were likely influenced by proteoglycan incorporation into collagen fibrils. Myocardial proteoglycans are known to be increased in response to POH but are not likely to be affected by the absence of SPARC. Therefore, the inclusion of proteoglycans by the PSR assay is likely to increase the apparent collagen fiber diameter as assessed by PSR, increase the measured collagen volume fraction and somewhat maximize (or perhaps overestimate) fibrillar collagen by the PSR assay. By contrast, hydroxyproline is specific to collagen molecules only. These three factors help explain why there were differences between CVF and hydroxyproline assessment of mature fully processed cross-linked myocardial fibrillar collagen and why the percent change in CVF was larger than that of the hydroxyproline assay. The hydroxyproline assay minimized (or perhaps underestimated) and the PSR assay maximized (or perhaps overestimated) the affects of the absence of SPARC on myocardial fibrillar collagen content. None the less, we believe that both the measurements of CVF and hydroxyproline are complimentary, that each measurement contributes to the overall understanding of collagen homeostasis in POH and confer an ability to examine the affects of SPARC on procollagen processing in POH. Importantly, both collagen measurements support the hypothesis that the absence of SPARC influences post-synthetic procollagen processing and alters collagen concentrations in the left ventricle both in the control state and after POH induced by TAC.

In previous studies, there has been some variability in the effects of pressure-overload on percent interstitial fibrosis, CVF, and collagen content (28–30). Variability in these measurements may be technique-dependent, based in part on whether PSR staining was performed with birefringence (polarized light) vs. without birefringence, whether Masson's trichrome staining was used, and the exact morphologic quantitation program used. PSR staining with birefringence stains only mature, fully processed cross-linked fibrillar collagen. PSR staining without birefringence is less specific for these collagen fibers. Masson's trichrome

stain binds to many types of ECM proteins and is not specific for fibrillar collagen. In addition, previous studies did not always state whether vasculature and epicardial surfaces were excluded from CVF measurements. For example in Zhang et. al. collagen volume fraction measured by quantification of LV myocardial sections stained with Masson's trichrome increased from ~1% in WT C57B16 mice to ~12% in POH mice (28). Zeisberg et al. reported ~20% fibrotic area in banded WT C57B16 mice, and Barrick et al. reported an increase from ~1% in normal mice to ~5% in POH mice in C57B16 mice (29,30). The measurements of CVF using PSR stained images in the current study are in close agreement to that of Barrick et al. It seems likely that the differences in ECM quantification as visualized by Masson's Trichrome versus PSR account for the range of values reported. Therefore, interpretation of our results and comparison with previously published results are dependent on a clear understanding of these methodological differences.

Myocardial Stiffness: Effects of the absence of SPARC

The increase in LV passive stiffness that occurred during POH was likely to be caused by changes in both the cardiomyocyte and the ECM. When ECM properties are altered, the remaining abnormalities in cardiomyocytes may still result in impaired LV diastolic function. When cardiomyocyte properties are altered, the remaining abnormalities in ECM may still result in impaired LV diastolic function. The data presented in previous studies and in the current study support this conclusion (16,17). The most important comparisons in the current study were those between WT control vs. WT TAC and between SPARC Null control vs. SPARC Null TAC. Examined in this fashion, the SPARC Null TAC had an increase in the insoluble collagen compared to SPARC Null control; however this increase was significantly less than in the WT mice. The same pattern was seen in the myocardial passive stiffness measurements. Therefore, the absence of SPARC did not completely normalize insoluble collagen or myocardial stiffness when SPARC Null TACs were compared to SPARC Null controls. These data support the conclusion that the increase in LV passive stiffness which occurred during POH was caused by abnormalities in both the cardiomyocyte and the ECM.

Systolic Function and Arterial Stiffness: Effects of the absence of SPARC

Data from the current study support the conclusion that the absence of SPARC did not affect arterial blood pressure or vascular compliance. These results are concordant with previous studies which demonstrate that systolic and diastolic blood pressure and arterial elastance are not significantly affected by the absence of SPARC (31). In addition, the absence of SPARC did not affect myocardial systolic properties, myocardial relaxation, or cardiomyocytes function. These data suggest that the effects of the absence of SPARC on myocardial fibrillar collagen primarily affect myocardial passive stiffness.

Limitations

Fibrillar collagen homeostasis is influenced by at least 3 regulatory control mechanisms: procollagen biosynthesis, post-synthetic procollagen processing, and collagen degradation (32–33). The balance between these three regulatory control mechanisms determines the total fibrillar collagen content present in a given pathological state at a specific time. The current study focused specifically on the role that SPARC plays in post-synthetic procollagen processing and facilitating the formation and assembly of mature cross-linked insoluble structural collagen fibrils. However, we recognize that experiments examining the effects of a change in SPARC on fibrillar collagen content must be interpreted in light of potential, simultaneous changes in the other regulatory control mechanisms.

In the TAC experiments, neither procollagen synthesis nor mature cross-linked collagen fibril degradation were directly measured, however, some of the data obtained in the current study and data from experiments performed in dermal fibroblasts suggests that the absence of SPARC

did not change either procollagen synthesis nor mature cross-linked collagen fibril degradation. For example, TAC induced PO increased total collagen to a similar extent in both WT and SPARC Null mice; the primary substantial differences were in the insoluble versus soluble collagen fractions which resulted in an increase in collagen content as measured by CVF and a change in fibrillar collagen morphology as evidenced in the scanning electron photomicrographs. In addition, data obtained from previous studies examining collagen synthesis and degradation in dermis and dermal fibroblasts showed no significant changes in collagen synthesis or degradation rates in SPARC Null vs. WT mice. While this conclusion will have to be supported by future studies that include direct *in vivo* measurements, data in the current study support the hypothesis that SPARC plays an important role in post-synthetic procollagen processing and facilitating the formation and assembly of mature cross-linked insoluble structural collagen fibrils.

The myocardial response to stress is dependent on the type of stress imposed (pressure overload, vs. volume overload vs. myocardial infarction), the strain of animal used, and the length over which the stress is imposed and the response monitored. Therefore, the affects of the absence of SPARC seen in the current study using TAC induced POH may differ if any of these variables are changed. One genetic background strain was used both in the SPARC Null and WT mice: C57Bl6/SV129. Thus at least this determinant of the response to the imposed stress was eliminated. The response to pressure overload will produce a different response than volume overload or myocardial injury from a myocardial infarction (MI). Whether procollagen processing and SPARC play an equivalent and important role in each type of stimulus is not fully known at this time. The current manuscript selectively examined the response to pressure overload. One previous study examined the response of SPARC-null mice to the imposition of an MI (34). In this study there was an 80% mortality rate after MI in SPARC-Null, whereas there was a 15% in the WT mice following an MI. In addition, following an MI, SPARC-Null mice developed misaligned and disorganized ECM. To date, no other published studies have examined the affect of the absence of SPARC in response to pressure overload, volume overload or MI. Future studies must be designed to fully evaluate the function of SPARC in post-synthetic procollagen processing in response to these different types of stimuli and the others factors listed above.

Whether there is a differential gender response to POH or the absence of SPARC has not been examined. In general, when the data were divided into male and female, the response appeared to be similar between genders. In particular, there appeared to be no gender differences in response to the absence of SPARC. However, this study was not powered with a sufficient sample size to perform a statistically valid comparison between genders. This question will require future studies.

Conclusions

Data from the current study support the following conclusions: 1) SPARC plays an important role in the post-synthetic procollagen processing in normal myocardium, 2) SPARC is significantly increased in pressure-overload myocardium, and 3) the absence of SPARC significantly alters the effects of pressure-overload on myocardial fibrillar collagen content and diastolic function. SPARC is one fundamental mechanism by which chronic PO increases myocardial fibrillar collagen content and contributes to the development of diastolic dysfunction. The regulation of SPARC and post-synthetic procollagen processing may provide important mechanism-based targets for the development of novel therapies for patients with CHF.

Supplementary Material

Refer to Web version on PubMed Central for supplementary material.

Acknowledgments

None

Funding Sources: This study was supported by the Research Service of the Department of Veterans Affairs (MR Zile, AD Bradshaw) and the National Heart, Lung, and Blood Institute Grants PO1-HL-48788 (MR Zile)

References

1. Chobanian AV, Bakris GL, Black HR, Cushman WC, Green LE, Izzo JL Jr, Jones DW, Materson BJ, Oparil S, Wright JT Jr, Roccella EJ, the National High Blood Pressure Education Program Coordinating Committee. The seventh report of the Joint National Committee on Prevention, Detection, Evaluation, and Treatment of High Blood Pressure. *JAMA* 2003;289:2560–2572. [PubMed: 12748199]
2. Lloyd-Jones DM, Larson MG, Leip EP, Beiser A, D'Agostino RB, Kannel WB, Murabito JM, Vasan RS, Benjamin EJ, Levy D. Lifetime risk for developing congestive heart failure. The Framingham Heart Study. *Circulation* 2002;106:3068–3072. [PubMed: 12473553]
3. Ahmed SH, Clark LL, Pennington WR, Webb CS, Bonnema DD, Leonardi AH, McClure CD, Spinale FG, Zile MR. Matrix metalloproteinases/tissue inhibitors of metalloproteinases: Relationship between changes in proteolytic determinants of matrix composition and structural, functional and clinical manifestations of hypertensive heart disease. *Circulation* 2006;113:2089–2096. [PubMed: 16636176]
4. Diez J, Querejeta R, Lopez B, Gonzalez A, Larman M, Martinez Ubago JL. Losartan-dependent regression of myocardial fibrosis is associated with reduction of left ventricular chamber stiffness in hypertensive patients. *Circulation* 2002;105:2512–2517. [PubMed: 12034658]
5. Solomon SD, Janardhanan R, Verma A, Bourgoun M, Daley WL, Purkayastha D, Lacourciere Y, Hippler SE, Fields H, Naqvi TZ, Mulvagh SL, Arnold JMO, Thomas JD, Zile MR, Aurigemma GP, the Valsartan in Diastolic Dysfunction (VALILDD) Investigators. Effect of angiotensin receptor blockade and antihypertensive drugs on diastolic function in patients with hypertension and diastolic dysfunction: A randomized trial. *Lancet* 2007;369:2079–2087. [PubMed: 17586303]
6. Martos R, Baugh J, Ledwidge M, O'Loughlin C, Conlon C, Patle A, Donnelly SC, McDonald K. Diastolic heart failure. Evidence of increased myocardial collagen turnover linked to diastolic dysfunction. *Circulation* 2007;115:888–895. [PubMed: 17283265]
7. Bishop JE, Laurent GJ. Collagen turnover and its regulation in the normal and hypertrophying heart. *Eur. Heart J* 1995;16:38–44. [PubMed: 7556271]
8. Bornstein P, Sage EH. Matricellular proteins: extracellular modulators of cell function. *Curr. Opin. Cell Biol* 2002;14:608–616. [PubMed: 12231357]
9. Bradshaw AD, Sage EH. SPARC, a matricellular protein that functions in cellular differentiation and tissue response to injury. *J. Clin. Invest* 2001;107:1049–1054. [PubMed: 11342565]
10. Rentz TJ, Poobalarahi F, Bornstein P, Sage EH, Bradshaw AD. SPARC regulates processing of procollagen I and collagen fibrillogenesis in dermal fibroblasts. *J. Biol. Chem* 2007;282:22062–22071. [PubMed: 17522057]
11. Bradshaw AD, Puolakkainen P, Dasgupta J, Davidson JM, Wight TN, Sage EH. SPARC-null mice display abnormalities in the dermis characterized by decreased collagen fibril diameter and reduced tensile strength. *J. Invest. Dermatol* 2003;120:949–55. [PubMed: 12787119]
12. Bradshaw AD, Reed MJ, Sage EH. SPARC-Null mice exhibit accelerated cutaneous wound closure. *J. Histochem. Cytochem* 2002;50:1–10. [PubMed: 11748289]
13. Puolakkainen P, Bradshaw AD, Kyriakides TR, Reed M, Brekken R, Wight T, Bornstein P, Ratner B, Sage EH. Compromised production of extracellular matrix in mice lacking secreted protein, acidic and rich in cysteine (SPARC) leads to a reduced foreign body reaction to implanted biomaterials. *Am. J. Pathol* 2003;162:627–635. [PubMed: 12547720]
14. Lang RM, Bierig M, Devereux RB, Flachskampf FA, Foster E, Pellikka PA, Picard MH, Roman MJ, Seward J, Shanewise JS, Solomon SD, Spencer KT, John Sutton M, Stewart WJ. Recommendations for Chamber Quantification: A Report from the American Society of Echocardiography's Guidelines and Standards Committee and the Chamber Quantification Writing Group, Developed in Conjunction

- with the European Association of Echocardiography, a Branch of the European Society of Cardiology. *J Am Soc Echocardiogr* 2005;18:1440–1463. [PubMed: 16376782]
15. Zile MR, Koide M, Sato H, Ishiguro Y, Conrad CC, Buckley JM, Morgan JP, Cooper G IV. Role of Microtubules in the contractile dysfunction of hypertrophied myocardium. *J Am Coll Cardiol* 1999;33:250–260. [PubMed: 9935038]
 16. Harris TS, Baicu CF, Conrad CH, Zile MR. Constitutive properties of hypertrophied myocardium: cellular contribution to changes in myocardial stiffness. *Am J Physiol* 2002;282:H2173–H2182.
 17. Stroud JD, Baicu CF, Barnes MA, Spinale FG, Zile MR. Viscoelastic properties of pressure overload hypertrophied myocardium: effect serine protease treatment. *Am J Physiol* 2002;282:H2324–2335.
 18. Blom AS, Mukherjee R, Pilla JJ, Lowry AS, Yarbrough WM, Mingoia JT, Hendrick JW, Stroud RE, McLean JE, Affuso J, Gorman RC, Gorman JH 3rd, Acker MA, Spinale FG. Cardiac support device modifies left ventricular geometry and myocardial structure after myocardial infarction. *Circulation* 2005;112(9):1274–1283. [PubMed: 16129812]
 19. Junqueira LC, Bignolas G, Brentani RR. Picosirius staining plus polarization microscopy, a specific method for collagen detection in tissue sections. *Histochem J* Jul;1979 11(4):447–55. [PubMed: 91593]
 20. Whittaker P, Kloner RA, Boughner DR, Pickering JG. Quantitative assessment of myocardial collagen with picosirius red staining and circularly polarized light. *Basic Res Cardiol* 1994;89(5):397–410. [PubMed: 7535519]
 21. Spinale FG, Tomita M, Zellner JL, Cook JC, Crawford FA, Zile MR. Collagen remodeling and changes in ventricular function during the development and regression of supraventricular tachycardia induced cardiomyopathy in swine. *Am J Physiol* 1991;261:H308–318. [PubMed: 1877659]
 22. Kregg JH, Hodgin JB, Hagaman JR, Smithies O. A noninvasive computerized tail-cuff system for measuring blood pressure in mice. *Hypertension* 1995;25:1111–1115. [PubMed: 7737724]
 23. Kelly RP, Ting CT, Yang TM, Liu CP, Maughan WL, Chang MS, Kass DA. Effective arterial elastance as index of arterial vascular load in humans. *Circulation* 1992;86:513–521. [PubMed: 1638719]
 24. Ishibashi Y, Takahashi M, Isomatsu Y, Qiao F, Iijima Y, Shiraishi H, Simsic JM, Baicu CF, Robbins J, Zile MR, Cooper G 4th. Role of microtubules versus myosin heavy chain isoforms in contractile dysfunction of hypertrophied murine cardiocytes. *Am J Physiol Heart Circ Physiol* 2003;285(3):H1270–85. [PubMed: 12750067]
 25. Lim CC, Apstein CS, Colucci WS, Liao R. Impaired cell shortening and relengthening with increased pacing frequency are intrinsic to the senescent mouse cardiomyocyte. *J Mol Cell Cardiol* 2000;32:2075–8202. [PubMed: 11040110]
 26. Zile MR, Richardson K, Cowles MK, Buckley JM, Koide M, Cowles BA, Gharpuray V, Cooper G 4th. Constitutive properties of adult mammalian cardiac muscle cells. *Circulation* 1998;98(6):567–79. [PubMed: 9714115]
 27. Prockop DJ, Kivirikko KI. Collagens: molecular biology, diseases, and potentials for therapy. *Ann. Rev. Biochem* 1995;64:403–434. [PubMed: 7574488]
 28. Zhang P, Xu X, Hu X, van Deel ED, Zhu G, Chen Y. Inducible nitric oxide synthase deficiency protects the heart from systolic overload-induced ventricular hypertrophy and congestive heart failure. *Circ Res* Apr 13;2007 100(7):1089–98. [PubMed: 17363700]
 29. Barrick CJ, Rojas M, Schoonhoven R, Smyth SS, Threadgill DW. Cardiac response to pressure overload in 129S1/SvImJ and C57BL/6J mice: temporal- and background-dependent development of concentric left ventricular hypertrophy. *Am J Physiol Heart Circ Physiol* 2007;292(5):H2119–30. [PubMed: 17172276]
 30. Zeisberg EM, Tarnavski O, Zeisberg M, Dorfman AL, McMullen JR, Gustafsson E, Chandraker A, Yuan X, Pu WT, Roberts AB, Neilson EG, Sayegh MH, Izumo S, Kalluri R. Endothelial-to-mesenchymal transition contributes to cardiac fibrosis. *Nat Med* Aug;2007 13(8):952–61. [PubMed: 17660828]
 31. Socha MJ, Manhiani M, Said N, Imig JD, Motamed K. Secreted Protein Acidic and Rich in Cysteine Deficiency Ameliorates Renal Inflammation and Fibrosis in Angiotensin Hypertension. *Am J of Path* 2007;171:1104–1112. [PubMed: 17717147]

32. Spinale FG. Myocardial matrix remodeling and the matrix metalloproteinases: Influence on cardiac form and function. *Physiol. Rev* 2007;87:1285–342. [PubMed: 17928585]
33. Nimni, ME. Fibrillar collagens: their biosynthesis, molecular structure, and mode of assembly. In: Zern, MA.; Reid, LM., editors. *Extracellular Matrix*. Marcel Dekker; New York: 1993. p. 121-148.
34. Schellings MW, van Loon M, Sage H, Pinto YM, Heymans S. Loss of SPARC Results in Increased Cardiac Rupture and Heart Failure After Acute Myocardial Infarction. *Circulation* 2006;114 (suppl):II-274.

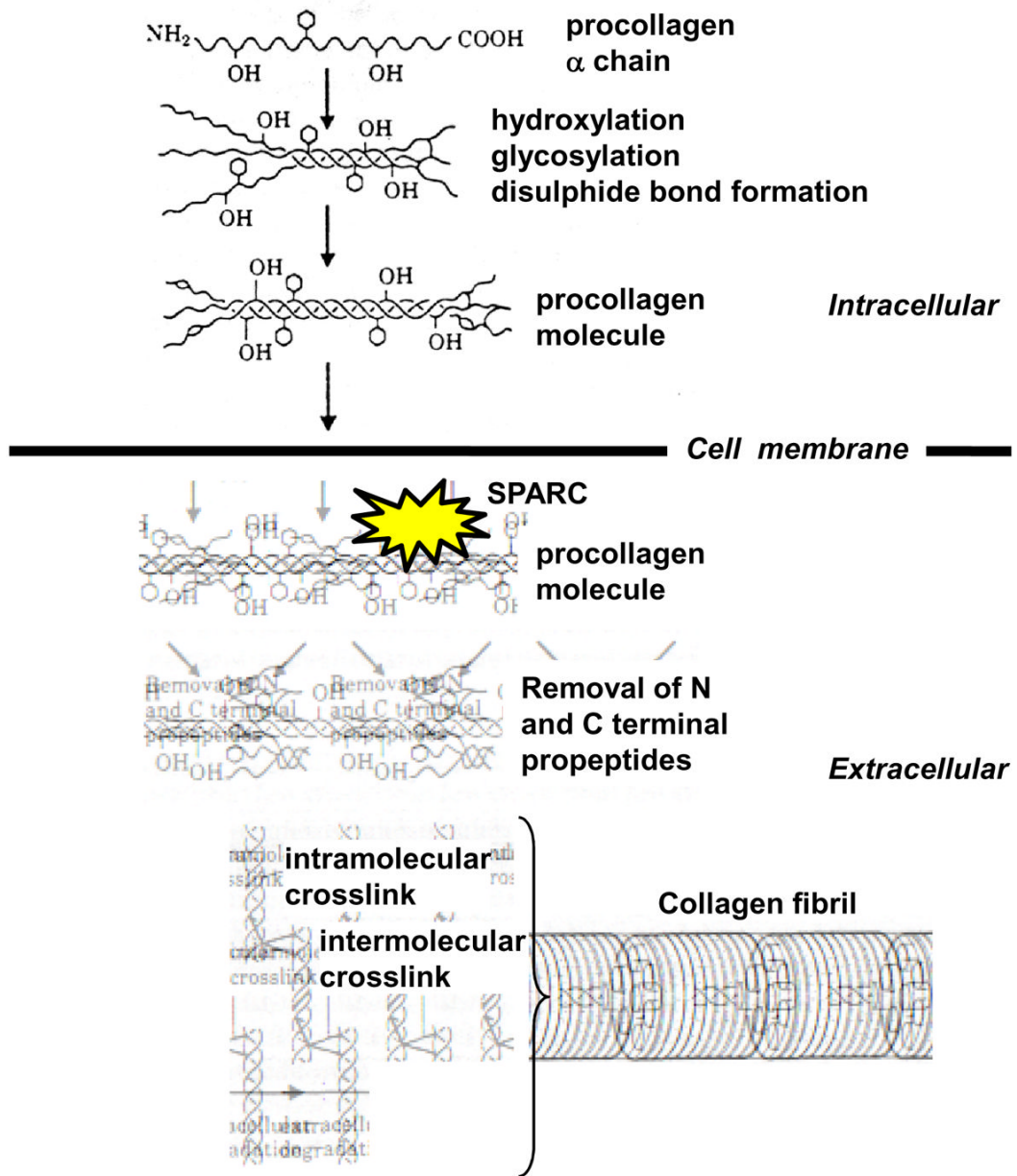


Figure 1. Schematic drawing representing intracellular steps of procollagen synthesis and extracellular steps of procollagen processing into a mature cross-linked collagen fibril. SPARC = Secreted Protein Acidic and Rich in Cysteine. SPARC, a procollagen binding protein with counter-adhesive activity, is hypothesized to participate in the coordination of procollagen processing and facilitate the formation and assembly of mature cross-linked insoluble structural collagen fibrils. (Modified with permission from reference 7)

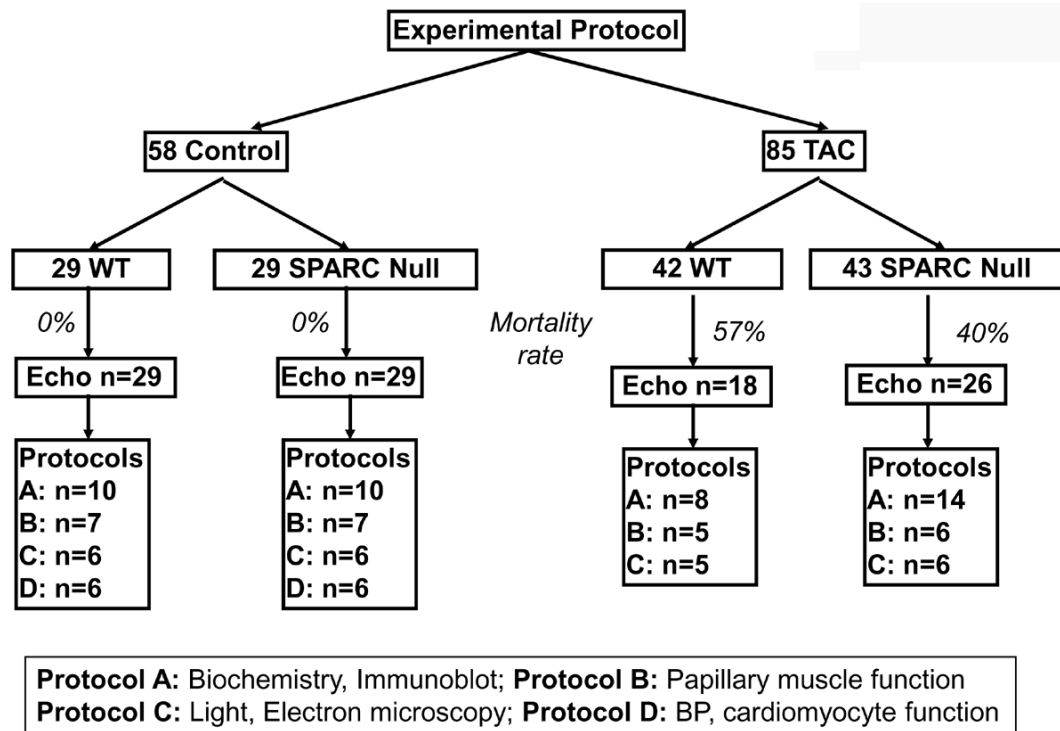


Figure 2.

Experimental protocol. WT = wild-type littermate mice C57Bl6/SV129, TAC = transverse aortic constriction, SPARC = Secreted Protein Acidic and Rich in Cysteine, SPARC Null = mouse created using targeted gene deletion to prevent expression of SPARC, Echo = echocardiogram, BP = blood pressure.

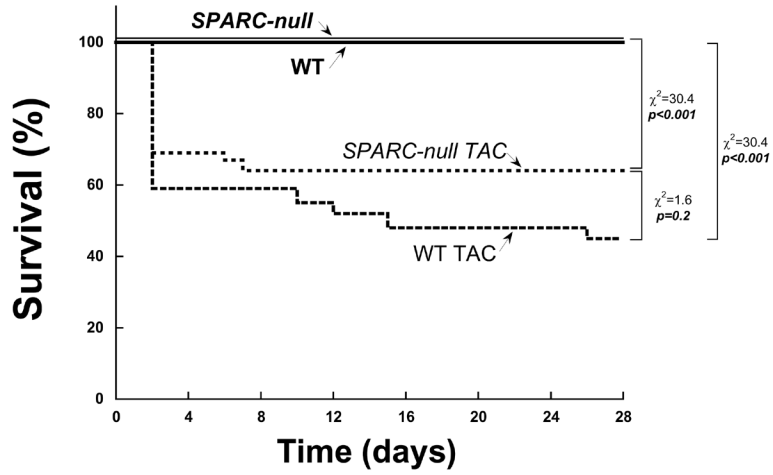


Figure 3.

Effects of the absence of SPARC (Secreted Protein Acidic and Rich in Cysteine) and the imposition of TAC (transverse aortic constriction) on mortality using a Kaplan-Meier analysis. WT = wild-type littermate mice C57Bl6/SV129, SPARC Null = mouse created using targeted gene deletion to prevent expression of SPARC. WT and SPARC Null control mice (that did not undergo TAC) received an echocardiogram at day zero and at day 28 (4 weeks). WT and SPARC Null TAC mice received an echocardiogram at day zero prior to TAC and at day 28 (4 weeks after TAC).

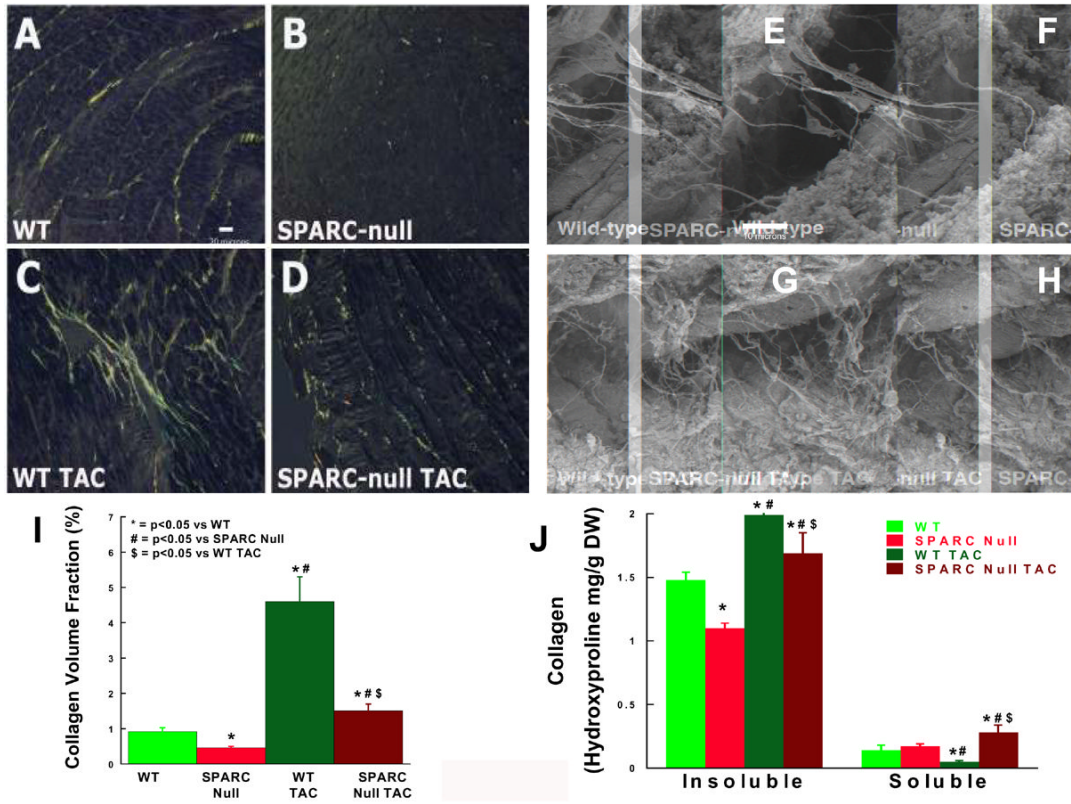


Figure 4. Effects of the absence of SPARC (Secreted Protein Acidic and Rich in Cysteine) and the imposition of TAC (transverse aortic constriction) on collagen content, composition and morphology. WT = wild-type littermate mice C57Bl6/SV129, SPARC Null = mouse created using targeted gene deletion to prevent expression of SPARC, * = $p < 0.05$ vs. WT, # = $p < 0.05$ vs. SPARC Null, & = $p < 0.05$ vs. WT TAC. Panels A–D, I: Collagen content was examined using picosirius red stained light microscopy to quantify collagen volume fraction. Scale bar = 20 microns. Panel J: Collagen composition was examined by measuring insoluble collagen vs. soluble collagen by hydroxyproline quantification. Panels E–H: Collagen morphologic structure was qualitatively examined using scanning electron microscopy. Scale bar = 10 microns.

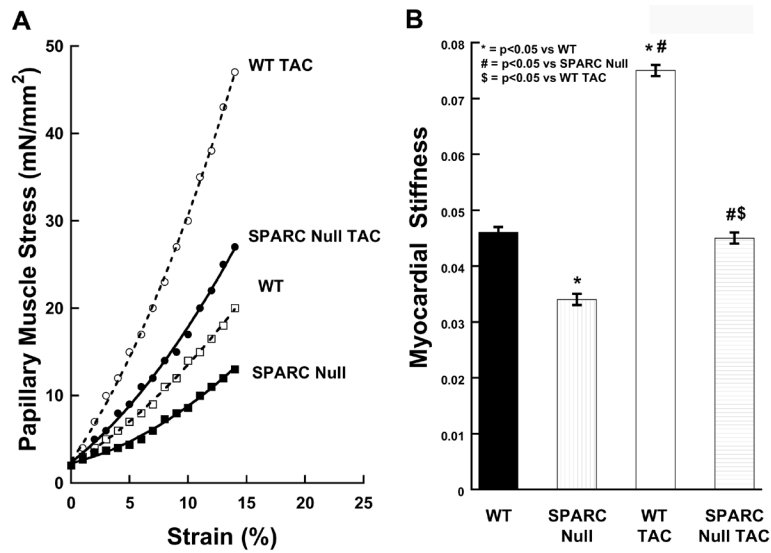


Figure 5.

Effects of the absence of SPARC (Secreted Protein Acidic and Rich in Cysteine) and the imposition of TAC (transverse aortic constriction) on myocardial diastolic stiffness. WT = wild-type littermate mice C57Bl6/SV129, SPARC Null = mouse created using targeted gene deletion to prevent expression of SPARC. * = $p < 0.05$ vs. WT, # = $p < 0.05$ vs. SPARC Null, & = $p < 0.05$ vs. WT TAC.

Panel A: Examples of the passive diastolic myocardial stress vs. strain curves for the four groups of animals studied: WT control, WT TAC, SPARC Null control, SPARC Null TAC. Panel B: Mean \pm SEM values of the passive stiffness constant, β , for the four groups of animals studied.

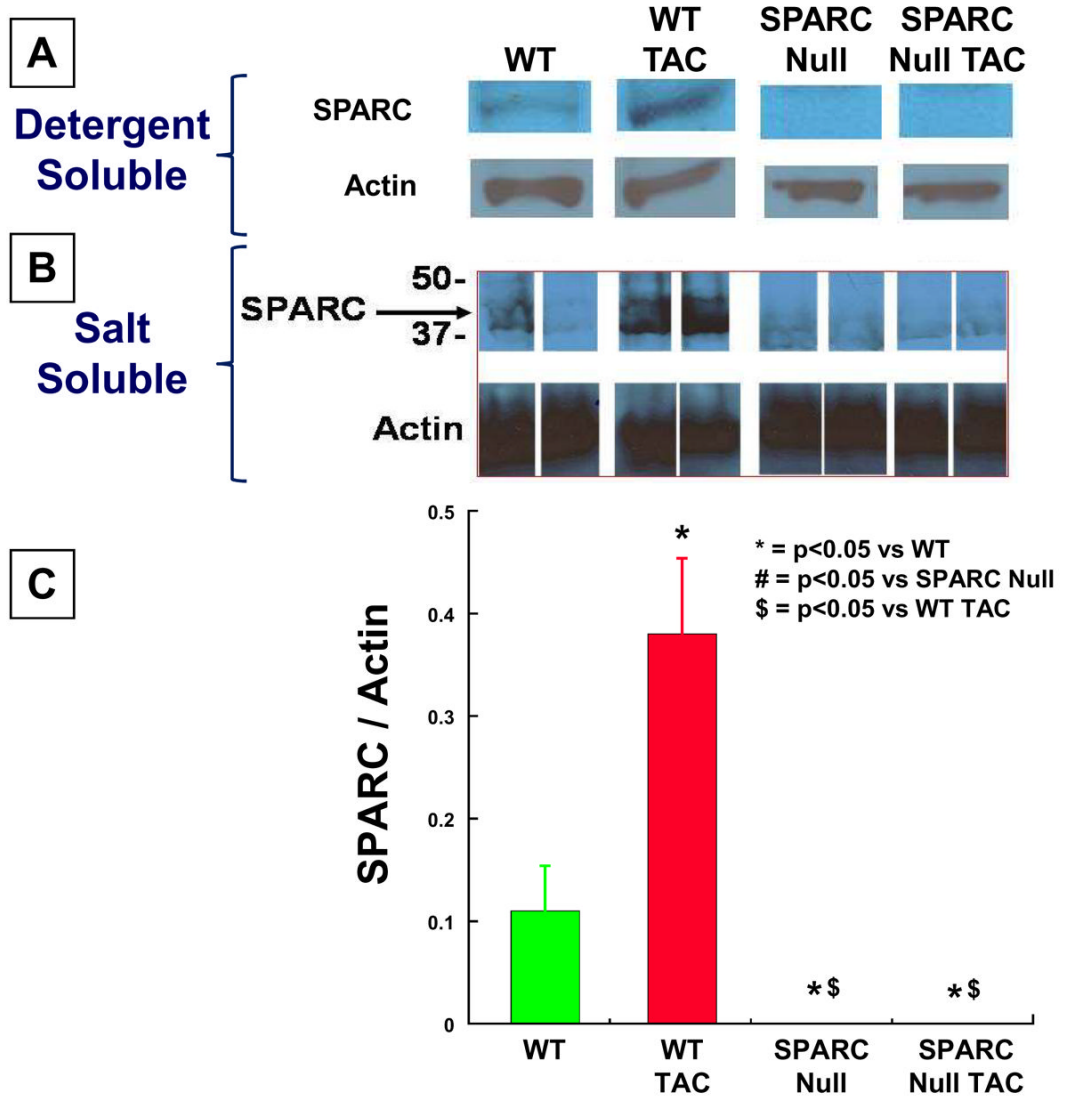


Figure 6. Immunoblots showing SPARC abundance from detergent soluble fraction (A) and Salt soluble fraction (B). Optical density analysis was used to semi-quantitate abundance for blots from n= 5 animals in each group. SPARC = Secreted Protein Acidic and Rich in Cysteine, TAC = transverse aortic constriction, WT = wild-type littermate mice C57Bl6/SV129, SPARC Null = mouse created using targeted gene deletion to abrogate expression of SPARC. * = p < 0.05 vs. WT, # = p < 0.05 vs. SPARC Null, \$ = p < 0.05 vs. WT TAC.

Table 1
Effects of TAC on LV Structure and Function in WT vs. SPARC Null Mice

	<u>Control</u>		<u>TAC</u>	
	WT	SPARC Null	WT	SPARC Null
Age (months)	4 ± 1	4 ± 1	4 ± 1	4 ± 1
BW (g)	25 ± 1	24 ± 1	22 ± 1	23 ± 1
Tibia Length (mm)	20 ± 1	20 ± 1	20 ± 1	20 ± 1
LV Mass (mg)	85 ± 5	88 ± 4	126 ± 8 [*]	136 ± 9 [#]
LV/BW (mg/g)	3.5 ± 0.1	3.6 ± 0.1	5.7 ± 0.3 [*]	5.9 ± 0.3 [#]
LV/TL (mg/mm)	4.2 ± 0.2	4.4 ± 0.2	6.3 ± 0.4 [*]	6.8 ± 0.4 [#]
AOPG (mmHg)	0	0	97 ± 3 [*]	97 ± 3 [#]
LV EDV (μL)	36 ± 1	38 ± 2	40 ± 2	38 ± 1
LV EF (%)	70 ± 3	72 ± 1	67 ± 2	70 ± 1
Wall Thickness (mm)	0.7 ± 0.1	0.7 ± 0.1	1.0 ± 0.1 [*]	1.1 ± 0.1 [#]
Heart Rate (bpm)	440 ± 18	426 ± 11	411 ± 25	403 ± 14

Abbreviations: AOPG = Aortic pressure gradient across the transverse aortic constriction (TAC), BW = Body Weight, EDV = End Diastolic Volume, EF = Ejection Fraction, LV = Left Ventricular, SPARC = Secreted Protein Acidic and Rich in Cysteine, TL = Tibia Length, WT = Wild Type, Data are mean ± SEM

* = p < 0.05 vs. Sham WT

= p < 0.05 vs. Sham SPARC Null, & = p <, 0.05 vs. WT TAC.

Table 2
Effects of TAC on Collagen Composition in WT vs. SPARC Null Mice

	<u>Control</u>		<u>TAC</u>	
	WT	SPARC Null	WT	SPARC Null
Total Collagen mg/gDW	1.63 ± 0.08	1.27 ± 0.04 [*]	2.01 ± 0.2 ^{*#}	1.96 ± 0.16 ^{*#}
Insoluble Collagen mg/gDW	1.48 ± 0.06	1.1 ± 0.04 [*]	1.99 ± 0.18 ^{*#}	1.69 ± 0.16 ^{*#} \$
% of Total	91 ± 1	87 ± 1 [*]	99 ± 2 ^{*#}	86 ± 2 ^{*\$}
Soluble Collagen mg/gDW	0.14 ± 0.04	0.17 ± 0.02	0.05 ± 0.01 ^{*#}	0.28 ± 0.06 ^{*#} \$
% of Total	9 ± 1	13 ± 1 [*]	1 ± 2 ^{*#}	14 ± 2 ^{*\$}

Abbreviations: Collagen is measured as Hydroxyproline, TAC = transverse aortic constriction, SPARC = Secreted Protein Acidic and Rich in Cysteine, Data are mean ± SEM

* = p < 0.05 vs. WT Control

= p <, 0.05 vs. SPARC Null

\$ = p <, 0.05 vs. WT TAC.

Table 3

Affects of the Absence of SPARC on Systolic and Diastolic Mechanical Properties

	<u>C57/129 WT</u>	<u>SPARC Null</u>
<i>Papillary Muscle</i>		
<u>Systolic Properties</u>		
Shortening percent	9.75 ± 1.08	9.66 ± 1.36
(-) dL/dt (mm/sec)	3.62 ± 0.81	3.72 ± 0.66
Peak Stress (mN/mm ²)	25.5 ± 6.6	26.0 ± 2.8
(+) dF/dt (mN/mm ² /sec)	343 ± 29	321 ± 31
<u>Diastolic Relaxation</u>		
(+) dL/dt (mm/sec)	2.98 ± 0.12	2.93 ± 0.16
(-) dF/dt (mN/mm ² /sec)	245 ± 25	271 ± 19
<i>Cardiomyocyte</i>		
<u>Systolic Properties</u>		
Percent Shortening (%)	10.1 ± 0.2	9.7 ± 0.2
Shortening Rate (µm/s)	258 ± 9	264 ± 8
<u>Diastolic Properties</u>		
Lengthening Rate (µm/s)	231.3 ± 7	236 ± 8
Passive stiffness (β)	9.1 ± 0.5	9.3 ± 0.6

Abbreviations: TAC = transverse aortic constriction, SPARC = Secreted Protein Acidic and Rich in Cysteine, (-) dL/dt = rate of muscle shortening, (+) dL/dt = rate of muscle lengthening, (+) dF/dt = rate of force development, (-) dF/dt = rate of force decline, Data are mean ± SEM, there were no significant differences between WT and SPARC Null.